HHS Public Access

Author manuscript

Oncogene. Author manuscript; available in PMC 2021 April 09.

Published in final edited form as:

Oncogene. 2020 December ; 39(49): 7181–7195. doi:10.1038/s41388-020-01497-4.

S6K1 blockade overcomes acquired resistance to EGFR-TKIs in non-small cell lung cancer

Hua Shen[1,2], **Gao-Chan Wang**[3], **Xiang Li**[3,4], **Xin Ge**[5], **Meng Wang**[3], **Zhu-Mei Shi**[5], **Vikas Bhardwaj**[6], **Zi-Xuan Wang**[3], **Ralph G. Zinner**[7], **Stephen C. Peiper**[3], **Andrew E. Aplin**[8], **Bing-Hua Jiang**[9], **Jun He**[3,*]

[1.]Department of Oncology, Sir Run Run Hospital, Nanjing Medical University, Nanjing, China

[2.]Department of Oncology, The First Affiliated Hospital of Nanjing Medical University, Nanjing, China

[3.]Department of Pathology, Anatomy & Cell Biology, Sidney Kimmel Cancer Center, Thomas Jefferson University, Philadelphia, USA

[4.]Department of Thoracic Surgery, First Affiliated Hospital of Xi'an Jiaotong University, Xi'an, China

[5.]Department of Pathology, State Key lab of Reproductive Medicine, Nanjing Medical University, Nanjing, China

[6.]College of Pharmacy, Thomas Jefferson University

[7.]Department of Medical Oncology, Thomas Jefferson University, Philadelphia, USA

[8.]Department of Cancer Biology, Sidney Kimmel Cancer Center, Thomas Jefferson University, Philadelphia, USA

[9.]Department of Pathology, Carver College of Medicine, University of Iowa, Iowa City, USA

Abstract

The development of resistance to EGFR Tyrosine kinase inhibitors (TKIs) in NSCLC with activating EGFR mutations is a critical limitation of this therapy. In addition to genetic alterations such as EGFR secondary mutation causing EGFR-TKI resistance, compensatory activation of signaling pathways without interruption of genome integrity remains to be defined. In this study, we identified S6K1/MDM2 signaling axis as a novel bypass mechanism for the development of EGFR-TKI resistance. The observation of S6K1 as a candidate mechanism for resistance to EGFR TKI therapy was investigated by interrogation of public databases and a clinical cohort to establish S6K1 expression as a prognostic/predictive biomarker. The role of S6K1 in TKI resistance was determined in *in vitro* gain-and-loss of function studies and confirmed in subcutaneous and orthotopic mouse lung cancer models. Blockade of S6K1 by a specific inhibitor PF-4708671

*Corresponding author: Jun He, Jun.he@jefferson.edu.

Conflicts of interest statement

All authors declare no potential conflicts of interest.

synergistically enhanced the efficacy of TKI without showing toxicity. The mechanistic study showed the inhibition of EGFR caused nuclear translocation of S6K1 for binding with MDM2 in resistant cells. MDM2 is a downstream effector of S6K1-mediated TKI resistance. Taken together, we present evidence for the reversal of resistance to EGFR TKI by the addition of small molecule S6K1/MDM2 antagonists that could have clinical benefit.

Keywords

S6K1; EGFR-TKI resistance; Non-small Cell lung cancer; PF-4708671; MDM2; Osimertinib

Introduction

Lung cancer is the leading cause of cancer-related mortality worldwide, which is responsible for one-third of all cancer death (1). Non-small-cell lung cancer (NSCLC) accounts for 85% of lung cancer cases in which only 15% of patients survive more than 5 year after the initial diagnosis (2). In addition to traditional treatments, targeted cancer therapies have emerged as a promising therapeutic strategy based on the pathogenesis of the disease. The epidermal growth factor receptor (EGFR) has been recognized as a landmark target of NSCLC therapy and thus EGFR tyrosine inhibitors (EGFR-TKIs) are widely used for NSCLC treatment. Patients with tumors bearing activating EGFR mutations benefit from treatment with EGFR-TKIs (3). However, in spite of this initial response, all responding patients eventually develop acquired resistance. The mechanisms can be either genetic alterations such as the acquisition of a second EGFR T790 mutation (4), or non-genetic changes such as small cell transformation, epithelial-mesenchymal transformation, and activation alternative signaling pathways *etc*. (5-9). However, the mechanisms involved in acquired EGFR-TKIs resistance remain unknown for 30% of clinical cases. In particular, the development of resistance to TKI for NSCLC with activating EGFR mutations is a critical limitation of this therapy (10, 11). Osimertinib has emerged as a third-generation irreversible TKI originally developed against the EGFR T790 mutation, and recently was approved as a first-line treatment of NSCLC patients with EGFR activating mutations (12). It was reported the acquired resistance to osimertinib as the first line is highly heterogeneous and mechanisms are quite distinct from those in patients treated with the first or second-generation TKI (13, 14).

Ribosomal protein S6 kinase 1 (S6K1, RPS6KB1, p70S6K1), a serine/threonine kinase, was initially discovered and cloned as the major kinase for mitogen-induced phosphorylation of the ribosomal S6 protein to promote global translation and cell growth (15). Several clinical studies found association between S6K1 overexpression and metastasis and poor prognosis in lung, colorectal, ovarian, and breast cancer (16-18). Moreover, a few studies indicated that S6K1 mediates drug resistance in colon cancer (19, 20). However, the role of S6K1 in EGFR-TKIs resistance had not been previously explored. In the current study, we demonstrate that persistent S6K1 signaling is engaged as a bypass mechanism for cancer cells to overcome EGFR inhibition through upregulating MDM2.

Materials and Methods

Cell culture, reagents, and antibodies

PC-9 cell line was obtained from the Type Culture Collection of the Chinese Academy of Sciences, Shanghai, China). PC-9/G cells (gefitinib resistant) were provided kindly by the Department of Oncology, Shanghai Pulmonary Hospital, Tongji University, Shanghai (21). HCC827 cells were obtained from ATCC (Manassas, VA, USA). All cell lines were authenticated by STR assay and showed no mycoplasma contamination confirmed by PCR-based assay. Gefitinib, erlortinib, osimertinib, PF-4708671, nutlin-3a and rapamycin were purchased from Selleck Chemicals (Houston, TX, USA). SP-141 was purchased from Cayman Chemical (Ann Arbor, MI, USA). AKT (#4691), p-S6 (#4858), p-AKT (#4060 CST), and S6K1 (#2708) antibodies were from Cell Signaling Technology. IGF-IR (sc463), p-IGF-IR (sc81499), TFEB (sc166736) antibodies were from Santa Cruz Biotech. p-TFEB antibody was obtained from Millpore Sigma (ABE1971). MDM2 antibodies were obtained from both Abcam (Ab243657) for IP and IHC application and from Cell Signaling Technology for Western-blots (#86934). Antibodies used for IHC or IF including p-S6K1 (AF3228), p-S6 (AF7331), p-4EBP1 (AF2308) and mTOR (AF6308) were purchased from Afinity Biosciences.

In vitro TKI resistance

HCC827-ER (erlotinib-resistant) and HCC827-OR (osimertinib-resistant) cells were established as described previously (22, 23). See details in Supplementary materials.

In vivo TKI resistance

Animal experimental protocols were in consistent with the Care and Use of Laboratory Animals Guide and approved by the Institutional Animal Care & Use Committee of Thomas Jefferson University (No. 01159). HCC827 cells were subcutaneously implanted into flanks of nude mice. When tumors reached around 100 mm^3 in size, mice were divided into three groups and were given osimertinib (2mg/kg), erlortinib (100 mg/kg), or solvent control by oral gavage daily (5 times a week). The treatments were discontinued when tumors in treated groups were gone after 3 to 4 weeks' administration. Mice in control group were terminated and tumors were excised for primary cell cultures. Tumor relapse occurred after a month and then TKIs were given until the treatments were unable to cause tumor shrinkage. The mice were then euthanized and tumors were removed for primary cell cultures. Isolation and maintenance of primary tumor cells were conducted using the Primary Cancer Culture System (PromoCell, Germany) according to the manufacturer's instructions.

Orthotopic lung cancer model in nude mice

PC-9/G cells stably expressing GFP were used to generate subcutaneous tumor in nude mice. Then tumor tissue was trimmed and cut into small pieces of 1 mm in diameter and stored in RPMI1640 medium. The trimmed tissues were transplanted into lungs by surgical orthotopic implantation. One week after tumor implantation, the mice were randomly divided into 5 groups by body weight without investigator blinding and treated with solvent control, gefitinib (200 mg/kg), osimertinib (2 mg/kg), gefitinib (200 mg/kg) plus

PF-4708671 (75 mg/kg), and osimertinib (2 mg/kg) plus PF-4708671(75 mg/kg). Gefitinib or osimertinib was given by oral gavage and PF-4708671 was given through intraperitoneal injection daily for 4 weeks. Tumor growth and metastasis were visualized by fluorescence imaging using Image-Pro Plus software 6.0 (Media Cybernetics Inc., Bethesda MD, USA).

Combination index

The combined effects of PF-4708671, TKI and SP-141 on resistant lung cancer cells were evaluated using the combination index (CI) as described previously (24, 25). In brief, the inhibitory level of chemicals was determined by MTT assay. The combination index was conducted using CompuSyn software (CompuSyn, Inc.). The combined effect is classified as follows: CI <0.9 indicates synergistic effect; 0.9 < CI < 1.1 indicated additive effect; CI >1.1 indicates antagonistic effect.

Immunofluorescence and immunohistochemistry

Cells were seeded on cover slips, and then treated with TKIs for 24 or 48 hours. The cells were fixed with 4 % formaldehyde in PBS buffer. After incubation with primary antibodies overnight, the FITC-labeled goat anti-rabbit or TRITC-labeled goat anti-mouse secondary antibody (Santa Cruz biotech, USA) was used to detect fluorescence. Cell nucleus was stained by Prolong Gold antifade reagent with DAPI (Invitrogen, CA, USA). IHC score was semi-quantified according to the percentage of positive cells and intensity of staining as previously described (26).

Human lung cancer tissue samples

Paraffin-embedded tumor samples of patients with NSCLC (n =51), who were receiving EGFR-TKI treatment, were collected from the Department of Pathology, First Affiliated Hospital of Nanjing Medical University, Jiangsu (China). The study protocol was approved by the Institutional Review Board of the First Affiliated Hospital of Nanjing Medical University (approval No. 2019-SR-260) with informed consent receiving from all patients. All samples were histologically classified and graded according to TNM stage by a clinical pathologist blinded to the outcome results. For survival analysis, the cut-off date was set for December, 2013.

Statistical Analysis

All results were obtained from at least three independent experiments. For animal experiments, 5–10 mice per group are typically used and treated for criteria achievement of statistical significance. Data are presented as mean ± SD from 3 independent experiments and analyzed by a two-tailed Student’s t-test. Differences were considered significant at a P value of ≤ 0.05. Data from GEO database and TCGA were retrieved and analyzed by R software. Survival data were analyzed by the Kaplan-Meier method using IBM SPSS Statistics 25 for Windows. The log-rank test was used to determine significant differences between overall survival curves.

Results

p-S6K1 is elevated in a NSCLC patient with acquired resistance to TKIs

A 39-year-old male patient was admitted to the hospital because of cough and body pain in November, 2017. The PET/CT examination showed left lung tumor with multiple metastases of liver, kidney, and bone metastasis (Fig.1A, left panel). The biopsy obtained by CT-guided liver puncture showed poorly differentiated adenocarcinoma. Genetic testing identified EGFR L858R point mutation, ALK wild-type, and no amplification of c-MET. The patient started treatments in January, 2018 with the following regime: Carboplatin + Bevacizumab + Erlortinib. Partial initial response was achieved after 2 months (Fig. 1A, middle panel). However, the patient eventually developed acquired resistance over time as reflected by the progressive disease (Fig.1A, right panel). The liver biopsy was re-obtained and no known EGFR secondary mutations such as T790M were detected. Immmuno-histochemistry staining for p-S6K1 was conducted using the liver puncture specimens. The specificity of p-S6K1 antibody was tested using kidney tissues from S6K1 knockout mice and wild-type mice kindly provided by Dr. Paul Fox at Cleveland Clinic (Fig.S1A). The p-S6K1 showed weak positive before the treatments and became strong positive by the time when tumors developed resistance (Fig.1B).

S6K1 phosphorylation levels are correlated with EGFR-TKI resistance and poor prognosis in NSCLC patients

Data retrieved from GEO database showed a significantly higher level of S6K1 in lung cancer tissues relative to normal lung tissues in a GEO dataset, especially in NSCLCs (Fig.2A). We conducted a survival analysis using the same dataset and TCGA dataset. Both results showed that high expression levels of S6K1 were linked with a shorter overall survival time (Fig.2B). We analyzed lung tumor specimens from NSCLC patients treated with EGFR-TKIs (gefitinib and erlortinib) (Suppl. Table 1), and retrospectively examined the clinical response and survival data from these patients. The tumor samples were collected before the TKI treatment. The criteria of specimen for analysis are: 1) The EGFR statuses of specimens were either exon 19 deletion or L858R mutation determined at the time of diagnosis; 2) There were no EGFR T790M detected in patients developed progressive disease after TKI treatment determined by ctDNA mutation analysis. Immunohistochemistry (IHC) assays were performed in formalin-fixed paraffin-embedded (FFPE) sections for p-S6K1 expression. Patients with progressive disease (PD) had higher expression levels of p-S6K1 compared to patients with partial response (PR) or stable disease (SD) (Fig.2C, 2D). Follow-up studies showed patients with higher p-S6K1 expression levels had shorter overall survival after EGFR-TKI treatment than those with lower p-S6K1 expression levels (Fig.2E). We also investigated the expression levels of p-S6, p-AKT and mTOR in the lung cancer specimens. As expected, p-S6 levels were higher in patients with progressive diseases; however, no significant difference was found in terms of p-AKT and mTOR expressions among groups (Fig.S1B). EGFR mutations may coexist with other gene mutations which have been reported as mechanisms of TKI resistance. We retrospectively analyzed mutation profiles of 11 ctDNA samples from patients who developed progress disease after TKI treatment. Next generation sequencing method was used to detect the common mutations that are related with TKI resistance. We found one

sample had PIK3CA mutation (p.H1047R Exon21) while another sample harbored *Met* amplification. Both tissue samples had strong p-S6K1 staining as shown in Fig.S1C. Although it is not clear at the current stage which mechanisms act dominantly in TKI resistance, S6K1 expression plays a role in EGFR mutant NSCLCs that also have other resistance mechanisms. Collectively, these data suggest that p-S6K1 expression levels are clinically relevant to the TKI resistance, and may act as a predictive biomarker for EGFR-TKI therapy.

S6K1 signaling is constitutively activated in resistant cancer cells upon EGFR-TKI treatments

To determine the role of S6K1 in EGFR-TKI resistance, we used three pairs of TKI sensitive versus resistant cell lines to explore the underlying molecular mechanism: PC-9 vs. PC-9/G, HCC827 vs. HCC827-ER, HCC827 vs. HCC827-OR. The PC-9 gefitinib resistant cells (PC-9/G) (kindly provided by Department of Oncology, Shanghai Pulmonary Hospital, Tongji University, Shanghai) established as described before (21, 27), were > 100 times more resistant to gefitinib than their parental PC-9 cells (Fig.S2A). No secondary mutation T790M or c-Met protein overexpression was found in PC-9/G cells (21). Notably, PC-9/G was also resistant to osimertinib; resistance was more than 22-fold higher in IC50 compared to PC-9 cells (Fig.S2B). We also used HCC827 cell line to develop erlortinib-resistant HCC827-ER and osimertinib-resistant HCC827-OR cells (Fig.S2C, S2D). The newly established resistant cell lines had the same mutation profile as the parental cell line using a Pan-cancer profiling analysis (42-gene panel, data not shown). In particular, no secondary EGFR mutation was detected.

As expected, EGFR signaling was effectively blocked by TKIs treatments as reflected by the loss or reduction of p-EGFR levels in both sensitive and resistant cells (Fig.3A, B, C, and D). Notably, we found that TKIs treatment almost diminished the p-S6K1 level in sensitive cells. In contrast, p-S6K1 signals were retained in resistant PC-9/G, HCC-827-ER, and HCC827-OR cells. To further confirm the above findings, we generated primary resistant cell lines from TKIs-resistant xenograft tumors in mice as detailed in the Methods (Fig.3E). Consistent with the results conducted in *vitro*, p-S6K1 disappeared in control tumor cells but was retained in resistant tumors when treated with osimertinib or erlortinib. (Fig.3F).

We then sought to explore the potential mechanisms underlying gefitinib-induced S6K1 activation in resistant cells. Gene copy number analysis showed no *S6K1* gene amplification in resistant PC-9/G cells (Fig. 3G). As S6K1 is typically regulated by activation of mTOR complex 1, we aimed to investigate if mTORC1 is activated, as evidenced by the phosphorylation of its two canonical downstream targets p-4EBP1 and p-TFEB. Similar as the result shown before, p-S6K1 signal was almost diminished in sensitive cancer cells upon TKI but retains in resistant cells, indicating a potential mechanism underlying TKI resistance. However, p-4EBP1, p-TFEB levels remain the same or slightly upregulated in sensitive cells upon TKI treatments, a pattern different than that in p-S6K1, suggesting that S6K1 activation is mTOR-independent (Fig.3H). AKT and IGF-IR pathways were reported to confer resistance to EGFR-TKIs (10, 28-31). We found that p-AKT was reduced by gefitinib in both cell lines, whereas p-IGF-IR was moderately increased in both sensitive and

resistant cells, suggesting a compensatory activation of IGF-IR signaling due to blockade of EGFR pathway (Fig.3I). Collectively, the results showed that the persistent S6K1 activation is not regulated through the canonical AKT/mTOR pathway.

S6K1 affects cell responsiveness to TKIs treatments *in vitro* and *in vivo*

To determine the role of S6K1 activity in gefitinib resistance, we overexpressed S6K1 in PC-9 cells through transient transfection with a S6K1 plasmid or a vector, or knocked down S6K1 in PC-9/G cells with a siRNA SMARTpool against S6K1. Cell viability assay showed that constitutive expression of S6K1 rendered PC-9 cells less susceptible to gefitinib, whereas knockdown of S6K1 made PC-9/G cells more sensitive to the treatment (Fig.4A). Then, we investigated whether S6K1 knockdown in PC-9/G cells promotes gefitinib-induced apoptosis. Active caspase-9 initiates apoptosis by cleaving and thus activating executioner caspases such as caspase-3, 6 and 7 (32). The ratio of cleaved caspase-9 versus total caspase 9 increased in S6K1 knockdown cells compared with the control when treated with gefitinib at the dose of 0.5 μM (Fig.4B). This result was further supported by the increase of cleaved-poly (ADP-ribose) polymerase (PARP) that is often associated with activation of caspases cascade (33). In similarity to the results obtained from western-blotting, immunofluorescence staining revealed that cleaved-caspase 3 expression level dramatically increased in knockdown cells in responds to gefitinib (Fig.S3A). We also established a HCC827 cell line stably expressing S6K1 (Fig.S3B). Overexpression of S6K1 limited the inhibitory effects of TKI on DNA synthesis as reflected by higher levels of cells in the S-phase fraction relative to those in the control vector cells (Fig.4C).

To determine whether S6K1 inhibition sensitizes resistant cancer cells to gefitinib treatment *in vivo*, PC-9/G cells that stably knocked-down *S6K1* were established using a shRNA approach (Fig. S3C). These cells were subcutaneously implanted in nude mice. PC-9/G control cells displayed gefitinib resistance properties while knockdown of *S6K1* resulted in small tumors in response to gefitinib treatment (Fig.4D, 4E, Fig.S3D). The results indicate that S6K1 confers acquired resistance to TKI, and that the development of S6K1-targeted therapeutics would be beneficial for a subset of NSCLCs patients.

S6K1 inhibition with PF-4708671 improves the efficacy of EGFR-TKIs both in *vitro* and in *vivo*

PF-4708671 was developed as the first S6K1 specific inhibitor and has been shown to reduce xenograft tumor growth in nude mice. Hence, we investigated whether PF-4708671 would improve the efficacy of TKI in NSCLCs *in vitro* and *in vivo* for the purpose of potential clinical application in the future. As expected, PF-4708671 effectively inhibited S6K1 activity in PC-9/G cells using an *in vitro* substrate-based kinase assay (Fig.5A). To address the concern about the potential toxicity, we treated normal immortalized bronchial epithelial Beas2B cells with PF-4708671 followed by cell viability assay and cell-cycle analysis. No significant change was observed in terms of cell proliferation and cell-cycle progression *in vitro* (Fig.S4A, B). PF-4708671 alone has been shown to reduce xenograft tumor growth in nude mice (34). We then investigated the effect of PF-4708671 on tumor growth *in vivo* by establishing subcutaneous xenografts in nude mice using HCC827 cells. However, administration of PF-4708671 showed limited efficacy to suppress tumor growth

compared with osimertinib. (Fig.S4C). To determine whether PF-4708671 can synergistically enhance the cytotoxicity of TKI in resistant cells, a MTT assay was used to examine the effects of PF and TKI on cell viabilities. More than 60% cells were still viable when treated with osimertinib or PF alone at the highest doses (Fig.5B, C). Notably, the combination of osimertinib and PF induced higher cytotoxicity in HCC827-OR cells (Fig.5D). The combination index (CI) analyzed by CompuSyn software showed the strong synergism between osimertinib and PF (Fig. 5E). Similar results were obtained in PC-9/G cells treated with gefitinib (Fig.S4D, E, F, G), indicating that PF-4708671 was able to re-sensitize resistant cells to TKI. Next, we examined the cell-cycle distributions of HCC827-ER cells when treated with erlortinib with or without PF-4708671. Erlortinib alone did not affect the cell-cycle progression, but the combination with PF-4708671 significantly reduced the S-phase fraction, and increased G_0-G_1 phase fraction meaning G_0-G_1 cell-cycle arrest (Fig.5F). We then carried out a flow-based apoptosis assay by Annexin V and PI staining in PC-9/G cells that are resistant to both gefitinib and osimertinib relative to its parental PC-9 cells. The percentage of early apoptotic cells treated with gefitinib or osimertinib plus PF-4708671 were about 26% and 23%, respectively, which were much higher than those in cells treated with TKIs alone (Fig.5G, Fig.S4H). To further investigate whether mTOR pathway is involved in S6K1-mediated TKI resistance, we treated PC-9/G cells with a mTOR inhibitor rapamycin, gefitinib, or the combo of rapamycin and gefitinib. The cell viability assay showed that the co-treatment with rapamycin and gefitinib exhibited an additive or even antagonistic effects as reflected by the combination index (Fig.S4I). We then investigate if rapamycin improve the efficacy of erlortinib on xenograft tumor growth in mice using HCC827-ER cells (Fig.S4J). We noticed that erlortinib inhibited tumor growth compared with the control. We figured the HCC827-ER cells generated *in vitro* were relatively resistant to erlortinib compared with the sensitive parental cells. Similar as the result show in Fig.S4C, PF alone didn't shrink the tumor but exhibited significant inhibitory effects with erlortinib treatment. Rapamycin moderately reduced the tumors but there was no significant difference in tumor weights between rapamycin alone and the combo with erlortinib, indicating that rapamycin couldn't improve the efficacy of TKIs (Fig.S4J).

To further evaluate if PF-4708671 can potentiate antitumor effects of EGFR-TKIs, we developed an orthotopic lung cancer model in nude mice using PC-9/G-GFP cells (Fig.6A). After the 4-week treatments, no significant difference regarding mice body weights was observed between treated groups (Fig. 6B), indicating that the addition of PF-4708671 did not cause severe side effects on mice. We noticed that tumors decreased moderately in size when treated with gefitinib or osimertinib alone albeit not significantly (cont vs gefitinib P=0.07, cont vs osimertinib P= 0.11). We reasoned that PC-9/G cells used in the animal model were relatively more resistant to TKI compared with the parental control cells. Tumors drastically reduced in volume and weight when treated with TKI and PF-4708671 compared with TKI treatments alone (Fig. 6C, D, and Fig.S4K). Notably, we found mice with metastatic tumor sites in the control group (3 out of 6), gefitinib group (2 out of 5), osimertinib group (2 out of 6), but none in the combination groups. Both results from *in vitro* and *in vivo* suggest that S6K1 inhibitor PF-4708671 can greatly improve the antitumor properties of EGFR-TKIs in resistant lung tumors. Immunohistochemistry analysis showed

p-S6K1 expression levels in mice tumor tissues were drastically lower in groups treated with PF while p-AKT and p-4EBP1 levels didn't seem to change among groups (Fig.6E).

MDM2 is a downstream effector of S6K1-mediated TKIs resistance

Our group previously found that S6K1 enhanced MDM2 phosphorylation and stability (35). Indeed, overexpression of S6K1 elevated both total and phosphor MDM2 protein levels, and knockdown of S6K1 lowered those expression levels (Fig.S5A). Gefitinib effectively abrogated both p-MDM2 and total MDM2 protein levels in sensitive PC-9/G cells, but not in resistant PC-9/G cells (Fig.7A). Similarly, when treated with osimertinib, we observed robust reduction of p-MDM2 and moderate decrease of total MDM2 levels only in sensitive HCC827 cells, but not in resistant HCC827-OR cells (Fig.7B). When we silenced S6K1 using a siRNA approach in PC-9/G cells, p-MDM2 decreased in response to Gefitinib (Fig.7C). Similarly, PF-4708671 suppressed gefinitib-induced p-MDM2 in resistant PC-9/G cells. No significant change was observed when treated with rapamycin. Prior studies showed that S6K1 shuttled from the cytoplasm to the nucleus upon stimulation, which was related to drug resistance (15, 16, 37). Indeed, we observed that p-S6K1 in nuclear fraction was upregulated with gefitinib treatment in PC-9/G cells (Fig.7D). It was previously reported that MDM2 is not only a substrate but also a binding partner of S6K1, which is promoted by genotoxic stress (36). We showed that p-S6K1 interacted with MDM2 through co-immunoprecipitation assay (Fig.7E). MDM2 is largely located in the nucleus where it is bound to p53 (38). We then examined the subcellular localization of p-S6K1 and MDM2 in response to TKI treatment. Immunofluorescence studies revealed p-S6K1 shuttled from cytoplasm to nucleus to bind with MDM2 upon gefitinib or osimertinib treatment (Fig.7F, Fig.S5B). Knock down of MDM2 promoted osimertinib-induced apoptosis and proliferation inhibition (Fig.7G, H), indicating that MDM2 is a functional effector of S6K1 in mediating EGFR-TKIs resistance.

MDM2 acts as an E3 ubiquitin ligase to promote p53 degradation (39). Blockade of interaction between p53 and MDM2 by the binding inhibitor nutlin-3a induced p73 expression in p53 mutant PC-9/G cells, and p53 expression in p53 wild-type HCC827-OR cells, respectively (Fig.S5C). However, there were no changes in p53 or p73 protein levels in cells treated with gefitinib, suggesting a p53-independent pathway in MDM2-mediated resistance. SP-141 was designed to induce MDM2 autoubiquitination and proteasomal degradation regardless of the p53 status in cells (40). We found that SP-141 synergistically enhanced the effect of osimertinib in HCC827-OR cells (Fig.S5D). Moreover, the combination of SP-141 and PF-4708671 greatly synergized with osimertinib to augment cytotoxicity of osimertinib (Fig.7I, Fig.S5E). Tissue analysis showed the expression level of MDM2 was inversely correlated with clinical outcomes (Fig.7J, K). Patients with higher MDM-2 expression levels had poor prognosis with EGFR-TKIs treatment than those with lower MDM-2 expression levels (Fig.7L). Moreover, the MDM2 protein levels are positively correlated with p-S6K1 levels (Fig. 7M). Taken together, MDM2 serves as a key effector of S6K1-mediated TKI resistance.

Discussion

As abnormal oncogenic activation of EGFR signaling is a key trigger in various cancers, application of TKIs has been widely used in cancer patients with EGFR mutations especially in lung cancer as first-line treatments (1, 41). However, these TKIs failed to elicit durable clinical benefit due to the development of acquired drug resistance in cancer cells after initial responses. In addition to gained new EGFR mutations, compensatory activation of signaling pathways without interruption of genome integrity are able to by-pass effects of EGFR-TKIs and thus cause therapeutic resistance. In this work, we provide the first evidence that S6K1, in addition to its role in cancer progression by promoting cancer cell growth as a downstream effector of mTOR, may contribute to acquired resistance to EGFR-TKI in NSCLCs.

S6K1 activation upon growth factor stimulation is typically mediated by the PI3K/AKT/TSC/mTOR pathway (42). A recent study identified that mTOR E2419K mutation as a novel resistance mechanism to EGFR TKI by analyzing paired EGFR-mutant lung tumor samples before and after EGFR TKI treatment (43). The downstream signaling such as p-S6K, pS6 and p-4EBP1 strongly expressed in cells harboring mTOR E2419K mutation was efficiently inhibited by mTOR antagonists but remained insensitive to erlortinib. In this study, we found that p-AKT was inhibited in both sensitive and resistant cells by TKI, suggesting that the persistent S6K1 activation only in resistant cells is irrelevant to AKT signaling. Moreover, mTOR was not activated as reflected by expression levels of p-4EBP1 anad p-TFEB. Except for PI3K/mTOR pathway, other mechanisms especially negative regulators might be involved in S6K1 regulation. For instance, it is possible that inactivation of phosphatases potentiates in TKIs-mediated S6K1 activation. One of the most abundant intracellular serine/threonine (Ser/Thr) phosphatases protein phosphatase 2A (PP2A) has been shown to bind and dephosphorylate S6K1 (44). It is not known if PP2A contribute to TKIs-induced S6K1 signaling, which are warranted for further investigation. Since S6K1 could be activated either by a specific mTOR mutation or mTOR-independent unknown mechanisms as a functional downstream effector, S6K1 antagonists could have clinical efficacy to overcome TKI resistance in a relatively larger subset of lung cancer patients.

So far, the cellular effects of S6K1 have been studied largely using a mTOR inhibitor rapamycin in laboratories. Given the role of mTORC1/S6K1 signaling in cancer and metabolic disease, this drug and its analogues have been widely used for clinical trials in various cancer types (54). However, the efficacy in general is low for two major reasons: one is that rapamycin induces immune suppression; the other is that it disrupts S6K1-mediated negative-feedback loop that regulates PI3K signaling (55). Our results showed that rapamycin could not improve the efficacy of TKI both *in vitro* and *in vivo*, suggesting S6K1 activation upon TKI is mTOR pathway-independent. PF-4708671, the first characterized small molecular inhibitor, is the most studied S6K1 inhibitor in cells and animal models (45). Inhibition of S6K1 by PF-4708671 was shown to limit tumorigenesis in breast cancer and lung cancer cells (34, 46). In this work, PF-4708671 significantly decreased TKI-mediated cell viability, increased apoptosis of resistant cells, and reduced tumor growth using an orthotopic lung cancer model. Given the promise of S6K1 as a therapeutic target

for cancer treatment, a few S6K1 inhibitors have been studied on clinical trials. For instance, LY2584702 tosylate was on two phase I trials for patients who had advanced solid tumors refractory to therapy (47, 48). However, both trials discontinued largely due to the intolerable toxicity. Since PF-4708671 showed high efficacy for EGFR-TKI resistant lung cancer without showing toxicity in cells and animal models in our project, it might warrant future trials in clinical settings.

Although the subcellular localization of S6K1 is predominantly cytoplasmic, S6Ks are predicted to have a nuclear localization signal (NLS) in the N-terminal, suggesting that these proteins might be located in the cell nucleus (49). However, mechanisms underlying regulation and function of the nucleo-cytoplasmic shuttling of S6K1 remain undefined. In the present work, we found that S6K1 localization has linked to EGFR-TKI resistance. Inhibition of EGFR caused nuclear translocation of S6K1 for binding with MDM2 in resistant cells. MDM2 is a negative regulator of tumor suppressor p53 through ubiquitin-mediated degradation (50). In addition to conveying its oncogenic function through degradation of p53, MDM2 can foster cell transformation and tumorigenesis independent of the p53 pathway as evidenced by the presence of amplified MDM2 coupled with non-functional and mutated p53 in cancers (51). In this study, we observed that constitutive activation of MDM2 in resistant cells is p53-independent. A number of MDM2 inhibitors have been on clinical trials for various diseases. However, most of these antagonists are designed to block the interphase between MDM2 and p53, and have low or no efficacy against cancer cells with mutant or deficient p53 (52) (53). A novel MDM2 inhibitor SP-141 was able to inhibit MDM2 expression and induce its autoubiquitination and proteasomal degradation regardless of p53 status (40). We found that the S6K1 inhibitor PF-4708671 and SP-141 synergistically enhanced TKI-mediated toxicity in resistant cells, providing one more actionable target to magnify the therapeutic effect of TKI.

Recently, osimertinib was approved as a first-line treatment of NSCLC patients with EGFR activating mutations (12). So far there is no target therapy for patients who develop resistance to osimertinib. More importantly, the mechanism of acquired resistance to osimertinib in patients receiving it as the first line are dramatically distinct from those receiving the first or second-generation TKI as the first line (13, 14). In this study, we established osimertinib resistance cell line in the absence of other known resistance mechanisms, and found that S6K1 inhibition was highly effective in osimertinib-resistant lung cancer cells, providing a potential strategy to overcome osimertinib resistance. To sum up, we provide evidence that the S6K1-MDM2 axis is a novel mechanism in acquired resistance to EGFR-TKI therapy in NSCLC. The demonstrated efficacy of S6K1 pharmacologic antagonists in *in vivo* model systems raises the possibility that this resistance pathway may have actionable targets for EGFR-targeted therapies in a subgroup of NSCLC patients.

Supplementary Material

Refer to Web version on PubMed Central for supplementary material.

Acknowledgements

We appreciate Jennifer Fisher Wilson (Science and Medical Writer, Thomas Jefferson University) for her help on English editing. We thank Dr. Paul Fox and Dr. Terenzi (Cleveland Clinic) for kindly providing S6K1 knockout mice tissues.

Funding

This work was supported by National Cancer Institute (R00 CA 215316, R01 CA232587, R01 CA160495), Natural Science Foundation of China (No. 81874230), Jiangsu Social Development Project (China, BE2018726), the Natural Science Foundation of Jiangsu Province (Grants No. BK20171484), the Project of Invigorating Health Care through Science, Technology, and Education (Jiangsu Provincial Medical Youth Talent QNRC2016856), the Summit of the Six Top Talents Program of Jiangsu Province (2017-WSN-179). Research reported in this publication utilized the Flow Cytometry Facility at Sidney Kimmel Cancer Center at Jefferson Health, which was supported by the NCI of the NIH (P30CA056036).

Reference List

(1). Rolfo C, Giovannetti E, Hong DS, Bivona T, Raez LE, Bronte G, et al. Novel therapeutic strategies for patients with NSCLC that do not respond to treatment with EGFR inhibitors. Cancer Treat Rev 2014;40:990–1004. [PubMed: 24953979]

(2). Wao H, Mhaskar R, Kumar A, Miladinovic B, Djulbegovic B. Survival of patients with non-small cell lung cancer without treatment: a systematic review and meta-analysis. Syst Rev 2013;2:10. [PubMed: 23379753]

(3). Lynch TJ, Bell DW, Sordella R, Gurubhagavatula S, Okimoto RA, Brannigan BW, et al. Activating mutations in the epidermal growth factor receptor underlying responsiveness of non-small-cell lung cancer to gefitinib. N Engl J Med 2004;350:2129–39. [PubMed: 15118073]

(4). Fujita Y, Suda K, Kimura H, Matsumoto K, Arao T, Nagai T, et al. Highly sensitive detection of EGFR T790M mutation using colony hybridization predicts favorable prognosis of patients with lung cancer harboring activating EGFR mutation. J Thorac Oncol 2012;7:1640–4. [PubMed: 22899358]

(5). Cappuzzo F, Marchetti A, Skokan M, Rossi E, Gajapathy S, Felicioni L, et al. Increased MET gene copy number negatively affects survival of surgically resected non-small-cell lung cancer patients. J Clin Oncol 2009;27:1667–74. [PubMed: 19255323]

(6). Donev IS, Wang W, Yamada T, Li Q, Takeuchi S, Matsumoto K, et al. Transient PI3K inhibition induces apoptosis and overcomes HGF-mediated resistance to EGFR-TKIs in EGFR mutant lung cancer. Clin Cancer Res 2011;17:2260–9. [PubMed: 21220474]

(7). Engelman JA, Zejnullahu K, Mitsudomi T, Song Y, Hyland C, Park JO, et al. MET amplification leads to gefitinib resistance in lung cancer by activating ERBB3 signaling. Science 2007;316:1039–43. [PubMed: 17463250]

(8). Guix M, Faber AC, Wang SE, Olivares MG, Song Y, Qu S, et al. Acquired resistance to EGFR tyrosine kinase inhibitors in cancer cells is mediated by loss of IGF-binding proteins. J Clin Invest 2008;118:2609–19. [PubMed: 18568074]

(9). Zhang Z, Lee JC, Lin L, Olivas V, Au V, LaFramboise T, et al. Activation of the AXL kinase causes resistance to EGFR-targeted therapy in lung cancer. Nat Genet 2012;44:852–60. [PubMed: 22751098]

(10). Oxnard GR, Arcila ME, Chmielecki J, Ladanyi M, Miller VA, Pao W. New strategies in overcoming acquired resistance to epidermal growth factor receptor tyrosine kinase inhibitors in lung cancer. Clin Cancer Res 2011;17:5530–7. [PubMed: 21775534]

(11). de Bruin EC, Cowell C, Warne PH, Jiang M, Saunders RE, Melnick MA, et al. Reduced NF1 expression confers resistance to EGFR inhibition in lung cancer. Cancer Discov 2014;4:606–19. [PubMed: 24535670]

(12). Romaniello D, Mazzeo L, Mancini M, Marrocco I, Noronha A, Kreitman M, et al. A Combination of Approved Antibodies Overcomes Resistance of Lung Cancer to Osimertinib by Blocking Bypass Pathways. Clin Cancer Res 2018;24:5610–21. [PubMed: 29967248]

(13). Leonetti A, Sharma S, Minari R, Perego P, Giovannetti E, Tiseo M. Resistance mechanisms to osimertinib in EGFR-mutated non-small cell lung cancer. Br J Cancer 2019;121:725–37. [PubMed: 31564718]

(14). Gray JE, Okamoto I, Sriuranpong V, Vansteenkiste J, Imamura F, Lee JS, et al. Tissue and Plasma EGFR Mutation Analysis in the FLAURA Trial: Osimertinib versus Comparator EGFR Tyrosine Kinase Inhibitor as First-Line Treatment in Patients with EGFR-Mutated Advanced Non-Small Cell Lung Cancer. Clin Cancer Res 2019;25:6644–52. [PubMed: 31439584]

(15). Fenton TR, Gout IT. Functions and regulation of the 70kDa ribosomal S6 kinases. Int J Biochem Cell Biol 2011;43:47–59. [PubMed: 20932932]

(16). Bostner J, Karlsson E, Eding CB, Perez-Tenorio G, Franzen H, Konstantinell A, et al. S6 kinase signaling: tamoxifen response and prognostic indication in two breast cancer cohorts. Endocr Relat Cancer 2015;22:331–43. [PubMed: 25972244]

(17). Ip CK, Yung S, Chan TM, Tsao SW, Wong AS. p70 S6 kinase drives ovarian cancer metastasis through multicellular spheroid-peritoneum interaction and P-cadherin/b1 integrin signaling activation. Oncotarget 2014;5:9133–49. [PubMed: 25193855]

(18). Lu Q, Wang J, Yu G, Guo T, Hu C, Ren P. Expression and clinical significance of mammalian target of rapamycin/P70 ribosomal protein S6 kinase signaling pathway in human colorectal carcinoma tissue. Oncol Lett 2015;10:277–82. [PubMed: 26171014]

(19). Grasso S, Tristante E, Saceda M, Carbonell P, Mayor-Lopez L, Carballo-Santana M, et al. Resistance to Selumetinib (AZD6244) in colorectal cancer cell lines is mediated by p70S6K and RPS6 activation. Neoplasia 2014;16:845–60. [PubMed: 25379021]

(20). Zhang Y, Wang Q, Chen L, Yang HS. Inhibition of p70S6K1 Activation by Pdcd4 Overcomes the Resistance to an IGF-1R/IR Inhibitor in Colon Carcinoma Cells. Mol Cancer Ther 2015;14:799–809. [PubMed: 25573956]

(21). Ju L, Zhou C, Li W, Yan L. Integrin beta1 over-expression associates with resistance to tyrosine kinase inhibitor gefitinib in non-small cell lung cancer. J Cell Biochem 2010;111:1565–74. [PubMed: 21053345]

(22). Wykosky J, Hu J, Gomez GG, Taylor T, Villa GR, Pizzo D, et al. A urokinase receptor-Bim signaling axis emerges during EGFR inhibitor resistance in mutant EGFR glioblastoma. Cancer Res 2015;75:394–404. [PubMed: 25432173]

(23). Phuchareon J, McCormick F, Eisele DW, Tetsu O. EGFR inhibition evokes innate drug resistance in lung cancer cells by preventing Akt activity and thus inactivating Ets-1 function. Proc Natl Acad Sci U S A 2015;112:E3855–E3863. [PubMed: 26150526]

(24). Ashton JC. Drug combination studies and their synergy quantification using the Chou-Talalay method--letter. Cancer Res 2015;75:2400. [PubMed: 25977339]

(25). Wang Y, Deng X, Yu C, Zhao G, Zhou J, Zhang G, et al. Synergistic inhibitory effects of capsaicin combined with cisplatin on human osteosarcoma in culture and in xenografts. J Exp Clin Cancer Res 2018;37:251. [PubMed: 30326933]

(26). Zhang C, Hao L, Wang L, Xiao Y, Ge H, Zhu Z, et al. Elevated IGFIR expression regulating VEGF and VEGF-C predicts lymph node metastasis in human colorectal cancer. BMC Cancer 2010;10:184. [PubMed: 20459642]

(27). Koizumi F, Shimoyama T, Taguchi F, Saijo N, Nishio K. Establishment of a human non-small cell lung cancer cell line resistant to gefitinib. Int J Cancer 2005;116:36–44. [PubMed: 15761868]

(28). Desbois-Mouthon C, Cacheux W, Blivet-Van Eggelpoel MJ, Barbu V, Fartoux L, Poupon R, et al. Impact of IGF-1R/EGFR cross-talks on hepatoma cell sensitivity to gefitinib. Int J Cancer 2006;119:2557–66. [PubMed: 16988945]

(29). Jacobsen K, Bertran-Alamillo J, Molina MA, Teixido C, Karachaliou N, Pedersen MH, et al. Convergent Akt activation drives acquired EGFR inhibitor resistance in lung cancer. Nat Commun 2017;8:410. [PubMed: 28871105]

(30). Jiang X, Sinnett-Smith J, Rozengurt E. Carbachol induces p70S6K1 activation through an ERK-dependent but Akt-independent pathway in human colonic epithelial cells. Biochem Biophys Res Commun 2009;387:521–4. [PubMed: 19615971]

(31). Qi HW, Shen Z, Fan LH. Combined inhibition of insulin-like growth factor-1 receptor enhances the effects of gefitinib in a human non-small cell lung cancer resistant cell line. Exp Ther Med 2011;2:1091–5. [PubMed: 22977626]

(32). McIlwain DR, Berger T, Mak TW. Caspase functions in cell death and disease. Cold Spring Harb Perspect Biol 2013;5:a008656. [PubMed: 23545416]

(33). Boulares AH, Yakovlev AG, Ivanova V, Stoica BA, Wang G, Iyer S, et al. Role of poly(ADP-ribose) polymerase (PARP) cleavage in apoptosis. Caspase 3-resistant PARP mutant increases rates of apoptosis in transfected cells. J Biol Chem 1999;274:22932–40. [PubMed: 10438458]

(34). Qiu ZX, Sun RF, Mo XM, Li WM. The p70S6K Specific Inhibitor PF-4708671 Impedes Non-Small Cell Lung Cancer Growth. PLoS One 2016;11:e0147185. [PubMed: 26771549]

(35). Fang J, Meng Q, Vogt PK, Zhang R, Jiang BH. A downstream kinase of the mammalian target of rapamycin, p70S6K1, regulates human double minute 2 protein phosphorylation and stability. J Cell Physiol 2006;209:261–5. [PubMed: 16883576]

(36). Lai KP, Leong WF, Chau JF, Jia D, Zeng L, Liu H, et al. S6K1 is a multifaceted regulator of Mdm2 that connects nutrient status and DNA damage response. EMBO J 2010;29:2994–3006. [PubMed: 20657550]

(37). Valovka T, Verdier F, Cramer R, Zhyvoloup A, Fenton T, Rebholz H, et al. Protein kinase C phosphorylates ribosomal protein S6 kinase betaII and regulates its subcellular localization. Mol Cell Biol 2003;23:852–63. [PubMed: 12529391]

(38). Park HS, Park JM, Park S, Cho J, Kim SI, Park BW. Subcellular localization of Mdm2 expression and prognosis of breast cancer. Int J Clin Oncol 2014;19:842–51. [PubMed: 24292333]

(39). Haupt Y, Maya R, Kazaz A, Oren M. Mdm2 promotes the rapid degradation of p53. Nature 1997;387:296–9. [PubMed: 9153395]

(40). Wang W, Qin JJ, Voruganti S, Srivenugopal KS, Nag S, Patil S, et al. The pyrido[b]indole MDM2 inhibitor SP-141 exerts potent therapeutic effects in breast cancer models. Nat Commun 2014;5:5086. [PubMed: 25271708]

(41). Juchum M, Gunther M, Laufer SA. Fighting cancer drug resistance: Opportunities and challenges for mutation-specific EGFR inhibitors. Drug Resist Updat 2015;20:12–28. [PubMed: 26021435]

(42). Jiang BH, Liu LZ. Role of mTOR in anticancer drug resistance: perspectives for improved drug treatment. Drug Resist Updat 2008;11:63–76. [PubMed: 18440854]

(43). Yu HA, Suzawa K, Jordan E, Zehir A, Ni A, Kim R, et al. Concurrent Alterations in EGFR-Mutant Lung Cancers Associated with Resistance to EGFR Kinase Inhibitors and Characterization of MTOR as a Mediator of Resistance. Clin Cancer Res 2018;24:3108–18. [PubMed: 29530932]

(44). Shin S, Wolgamott L, Yu Y, Blenis J, Yoon SO. Glycogen synthase kinase (GSK)-3 promotes p70 ribosomal protein S6 kinase (p70S6K) activity and cell proliferation. Proc Natl Acad Sci U S A 2011;108:E1204–E1213. [PubMed: 22065737]

(45). Pearce LR, Alton GR, Richter DT, Kath JC, Lingardo L, Chapman J, et al. Characterization of PF-4708671, a novel and highly specific inhibitor of p70 ribosomal S6 kinase (S6K1). Biochem J 2010;431:245–55. [PubMed: 20704563]

(46). Khotskaya YB, Goverdhan A, Shen J, Ponz-Sarvise M, Chang SS, Hsu MC, et al. S6K1 promotes invasiveness of breast cancer cells in a model of metastasis of triple-negative breast cancer. Am J Transl Res 2014;6:361–76. [PubMed: 25075253]

(47). Hollebecque A, Houede N, Cohen EE, Massard C, Italiano A, Westwood P, et al. A phase Ib trial of LY2584702 tosylate, a p70 S6 inhibitor, in combination with erlotinib or everolimus in patients with solid tumours. Eur J Cancer 2014;50:876–84. [PubMed: 24456794]

(48). Tolcher A, Goldman J, Patnaik A, Papadopoulos KP, Westwood P, Kelly CS, et al. A phase I trial of LY2584702 tosylate, a p70 S6 kinase inhibitor, in patients with advanced solid tumours. Eur J Cancer 2014;50:867–75. [PubMed: 24440085]

(49). Tavares MR, Pavan IC, Amaral CL, Meneguello L, Luchessi AD, Simabuco FM. The S6K protein family in health and disease. Life Sci 2015;131:1–10. [PubMed: 25818187]

(50). Eischen CM. Role of Mdm2 and Mdmx in DNA repair. J Mol Cell Biol 2017;9:69–73. [PubMed: 27932484]

(51). Feeley KP, Adams CM, Mitra R, Eischen CM. Mdm2 Is Required for Survival and Growth of p53-Deficient Cancer Cells. Cancer Res 2017;77:3823–33. [PubMed: 28576884]

(52). Vassilev LT, Vu BT, Graves B, Carvajal D, Podlaski F, Filipovic Z, et al. In vivo activation of the p53 pathway by small-molecule antagonists of MDM2. Science 2004;303:844–8. [PubMed: 14704432]

(53). Shangary S, Qin D, McEachern D, Liu M, Miller RS, Qiu S, et al. Temporal activation of p53 by a specific MDM2 inhibitor is selectively toxic to tumors and leads to complete tumor growth inhibition. Proc Natl Acad Sci U S A 2008;105:3933–8. [PubMed: 18316739]

(54). Bilanges B, Vanhaesebroeck B. A new tool to dissect the function of p70 S6 kinase. Biochem J 2010;431:e1–e3. [PubMed: 20874709]

(55). Wan X, Harkavy B, Shen N, Grohar P, Helman LJ. Rapamycin induces feedback activation of Akt signaling through an IGF-1R-dependent mechanism. Oncogene 2007;26:1932–40. [PubMed: 17001314]

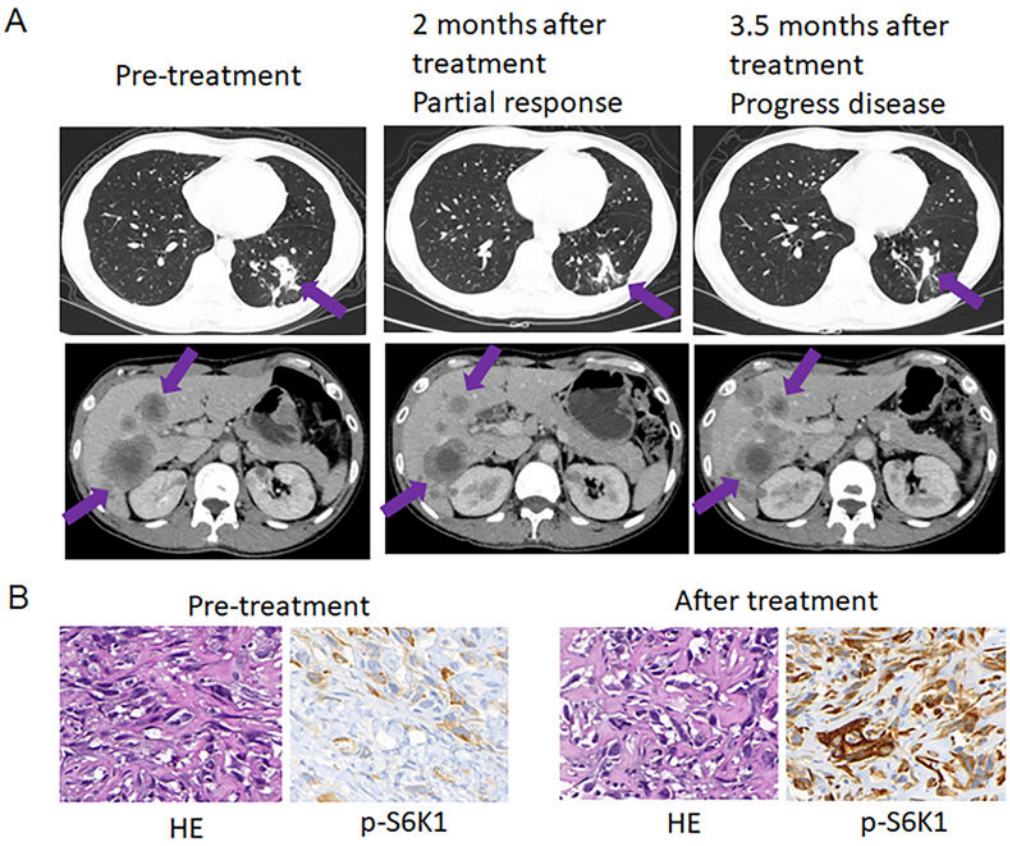

Fig.1. p-S6K1 is elevated in a NSCLC patient with acquired resistance to TKIs

(A) PET/CT lung tumor images before and after treatments. (B) p-S6K1 staining and HE staining in tumor specimens from the same patient before and after treatments. Magnification: × 200

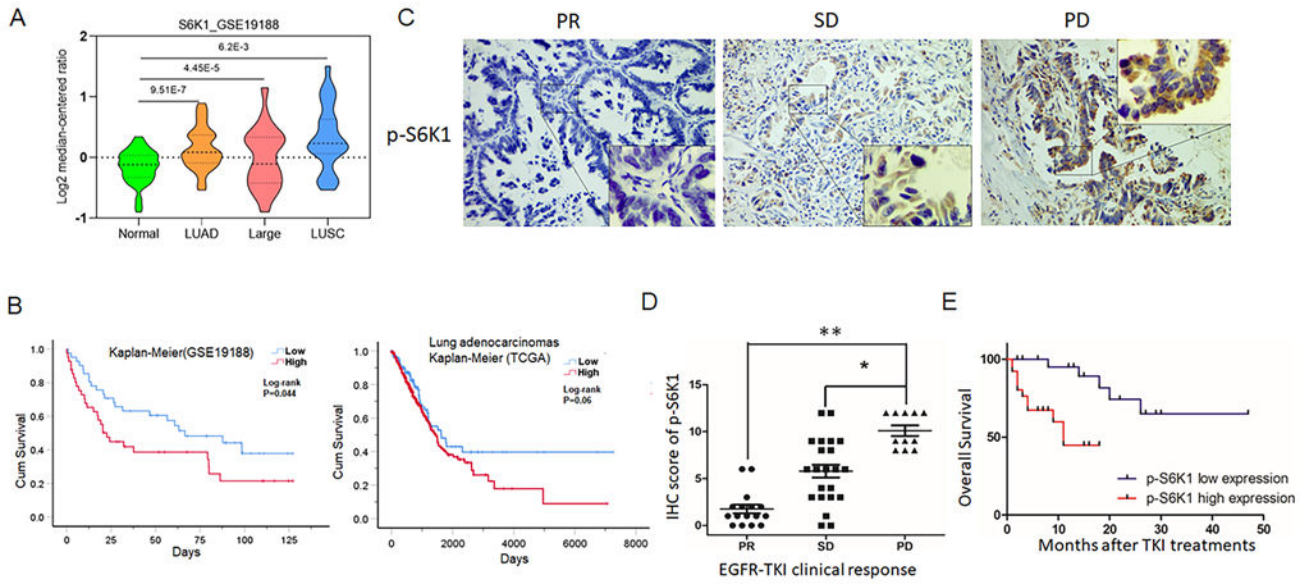

Fig.2. phosphorylation levels are correlated with EGFR-TKI resistance and poor prognosis in NSCLC patients

(A) High expression level of S6K1 in NSCLC. Data retrieved from GEO database (GSE19188). Normal (normal lung tissues), n= 65; LUAD (lung adenocarcinoma), n=45; Large (large cell carcinoma), n=19; LUSC (lung squamous carcinoma), n=27. (B) S6K1 expression levels are correlated with poor survivals in NSCLC. Left panel: data retrieved from GEO database (GSE19188). Low (low S6K1), n=41; High (high S6K1 (n=41). The median was used as a cut-off value. Right panel: data retrieved from TCGA database. Low: n= 125 High: n=375. Cut-off value=4.08. (C) Total 51 lung tumor specimens from NSCLC patients treated with EGFR-TKIs (gefitinib and erlortinib) were analyzed. The specimens were collected before TKI therapy. The EGFR statuses of specimens were either exon 19 deletion or L858R mutation determined at the time of diagnosis. There were no EGFR T790M detected after TKI treatment determined by ctDNA analysis. Representative images of p-S6K1 staining (× 200 and × 650 magnifications) were shown based on clinical response to EGFR-TKIs. PR: partial response; SD: stable disease; PD: progressive disease. (D) Correlation analysis was performed between p-S6K1 expression levels and clinical responses. PR (n=16), SD (n=25), PD (n=10). Quantitative results were analyzed by one-way ANOVA *P<0.05, ** P<0.01. (E) Kaplan-Meier curves were used to show overall survival of NSCLCs patients stratified based on the expression levels of p-S6K1. The cutoff of value of subgroups (low, high) of p-S6K1 expression level was the 50% percentile value. Log rank P<0.01.

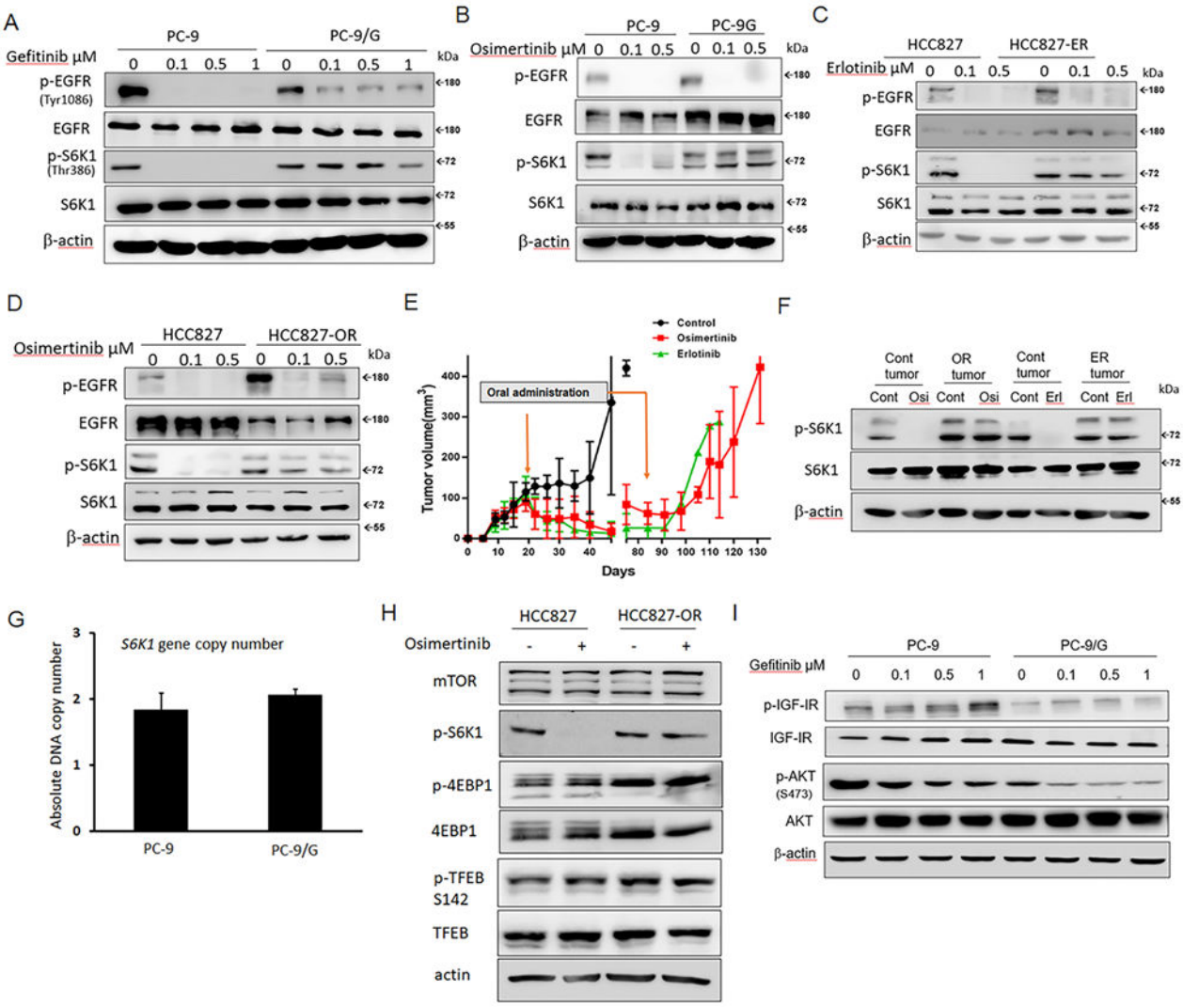

Fig.3. Persistent activation of S6K1 signaling in acquired resistant non-small lung cancer cells with EGFR-TKIs treatments

(**A, B, C, D**) Cells were treated with EGFR-TKIs for 1 hour at indicated doses and then subject to Western-blots. (**E**) Established primary resistant cell lines derived from tumors (n=5/group). Relapsed tumor occurred 2 out of 5 mice in osimertinib group and 1 out of 6 mice in erlortinib group. Tumor growth curves were shown. Tumor volumes are shown as mean ± SD. (**F**) Primary cell lines derived from control tumors, resistant tumors were treated with osimertinib (OR tumor), and erlotinib (ER tumor) for 1 hour respectively. The protein samples were prepared and subject to Western-blots assay. (**G**) Genomic DNAs were prepared from PC-9 and PC-9/G cells. S6K1 gene copy number analysis was performed as described in Methods. (**H, I**) Cells were treated with EGFR-TKI for 1 hour at indicated doses and then subject to Western-blots.

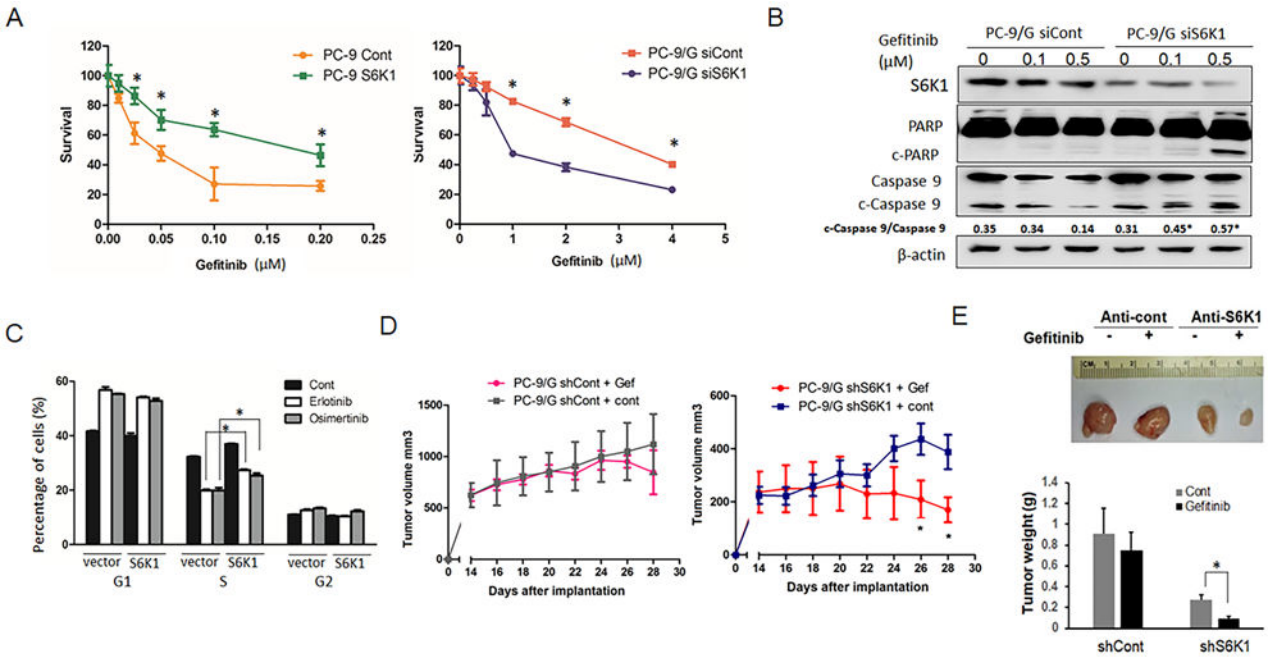

Fig.4. S6K1 affects cell responsiveness to TKIs treatments in NSCLC cells.

(**A**) PC-9 cells were transiently transfected with S6K1 or a vector control, and PC-9/G cells were transiently transfected with siS6K1 SMARTPOOL or siRNA scrambled control respectively. After 24 hours of transfection, the cells were treated with gefitinib at indicated doses for 72 hours. Cell viability was assessed by CCK8 assay. (**B**) PC-9/G cells were transiently transfected siS6K1 SMARTPOOL or vector control respectively. After 24 hours transfection, the cells were treated with gefitinib for 48 hours followed by Western blotting. (**C**) HCC827 vector and HCC827 S6K1 overexpressing cells were treated with erlortinib (0.1 μM) or osimertinib (0.1 μM) for 72 hours, and then were prepared for cell-cycle analysis. (**D)** Xenograft tumor growth curves were shown after implantation (n = 10/group). *P<0.05. (**E)** Left panel: representative image of tumors for each group; Right panel: Tumor volume (volume = $W^2 \times L \times 0.52$, where W is tumor width and L is tumor length) were measured and expressed as mean ± SEM. Quantitative results were analyzed by Student's t test (two groups) or one-way ANOVA (more than two groups) with $P \leq 0.05$ considered significant and are shown as mean ± SD. *P<0.05. For cell viability assay, three independent experiments were performed with 8-10 technical replicates for each treatment.

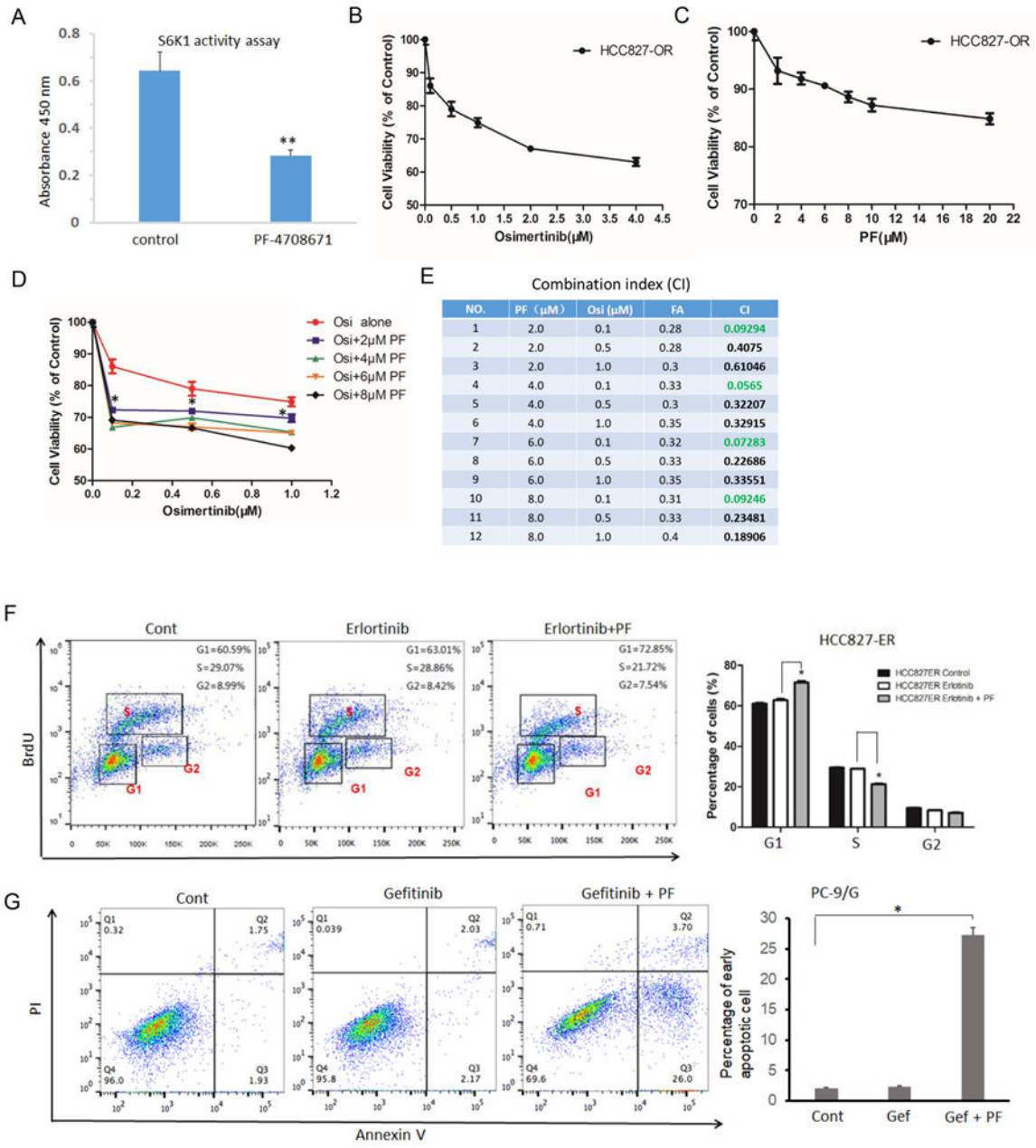

NO.	PF (μM)	Osi (μM)	FA	CI
1	2.0	0.1	0.28	0.09294
2	2.0	0.5	0.28	0.4075
3	2.0	1.0	0.3	0.61046
4	4.0	0.1	0.33	0.0565
5	4.0	0.5	0.3	0.32207
6	4.0	1.0	0.35	0.32915
7	6.0	0.1	0.32	0.07283
8	6.0	0.5	0.33	0.22686
9	6.0	1.0	0.35	0.33551
10	8.0	0.1	0.31	0.09246
11	8.0	0.5	0.33	0.23481
12	8.0	1.0	0.4	0.18906

Fig.5. S6K1 inhibitor PF-4708671 enhanced TKI-induced cytotoxicity *in vitro*

(A) Cell lysates were prepared from PC-9/G cells treated with PF-4708671 (4 μM) for 24 h for testing S6K1 activities. The kinase activity assay was performed using the assay kit from Enzo Life Sciences. **(B, C, D)** HCC827-OR cells were treated with osimertinib, PF-4708671, or combination of osimertinib and PF at indicated doses for 24 hours. MTT assay was performed to assess cell viability. All combination groups reduced cell viability when compared with osimerinib alone. *P<0.05. **(E)** The combination index was calculated by CompuSyn software. (**F**) HCC827-ER cells were treated with erlortinib (0.1 μM) with or without PF-4708671 (4 μM) for 72 hours followed by cell-cycle analysis. The percentage of cells in G1, S, and G2 were quantified. *P<0.05. (**G**) PC-9/G cells were treated with

gefitinib (0.5 μM) with or without PF 4708671 (4 μM) for 48 hours. Flow-based apoptosis assay was performed after Annexin V and PI staining. Percentage of early apoptotic cells were quantified. Data are presented as mean ± SE from 3 independent experiments. *P<0.05.

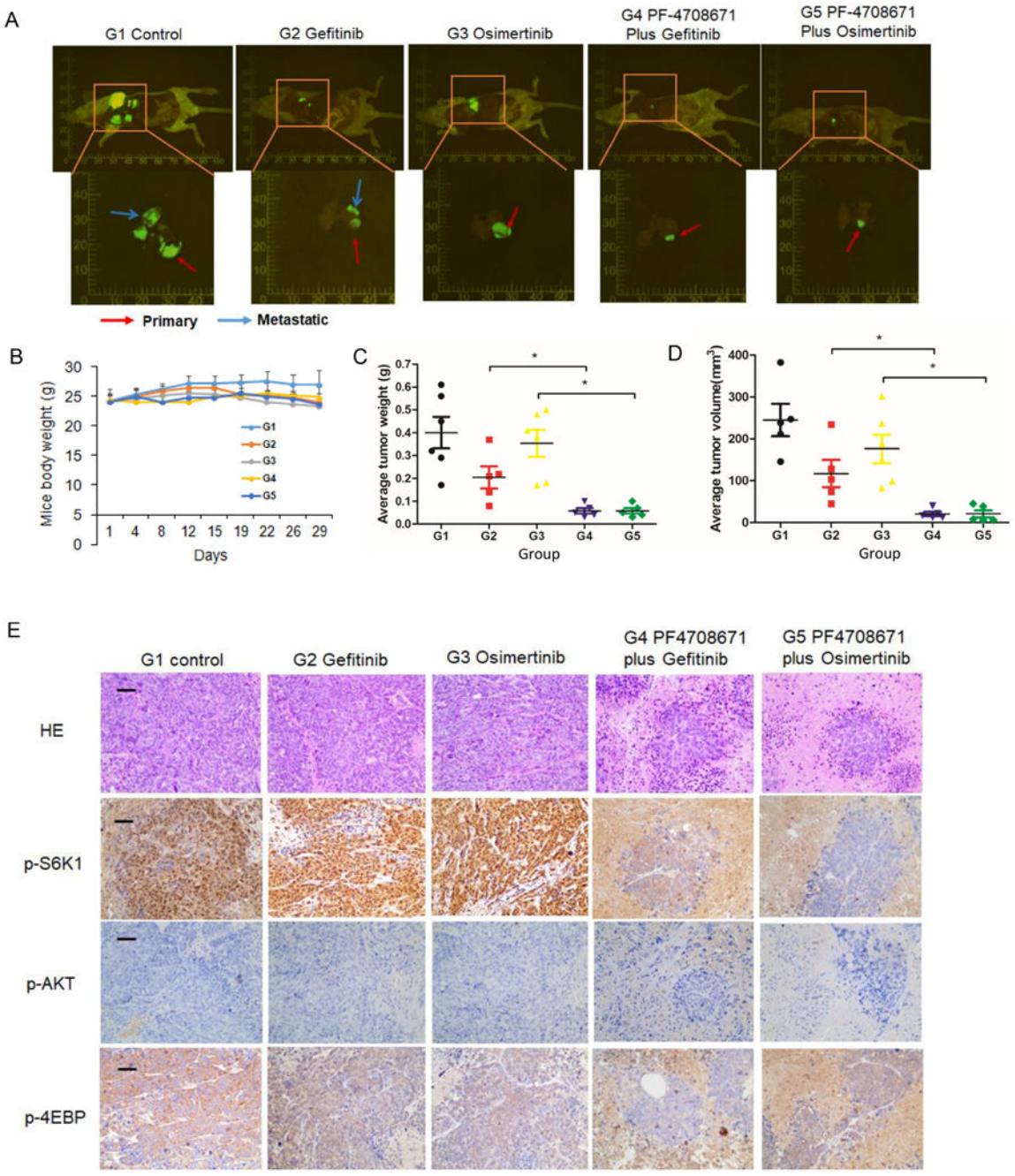

Fig.6. PF-4708671 improves the efficacy of EGFR-TKIs *in vivo*

(A) Orthotopic lung cancer model in nude mice was established using PC-9/G-GFP cells. Representative images of mice for each group were shown. Red arrow: primary tumor sites; blue arrow: metastatic tumor sites. (**B**) Mice weight in each group during the treatment was shown. (**C, D**) Quantification of tumor weight and volume for each group was shown. n =6 (G1, G3, G4, G5), n = 5 (G2). (**E**) Tumor tissues from mice were stained with HE and analyzed for p-S6K1, p-AKT, and p-4EBP1 by IHC methods. Representative images are shown. Magnification: 100×. Scale bar: 100 μm. Quantitative results were analyzed by Student's t test (two groups) or one-way ANOVA (more than two groups) with $P \leq 0.05$

considered significant and are shown as mean ± SD. *P<0.05. For cell viability assay, three independent experiments were performed with 6-8 technical replicates for each treatment.

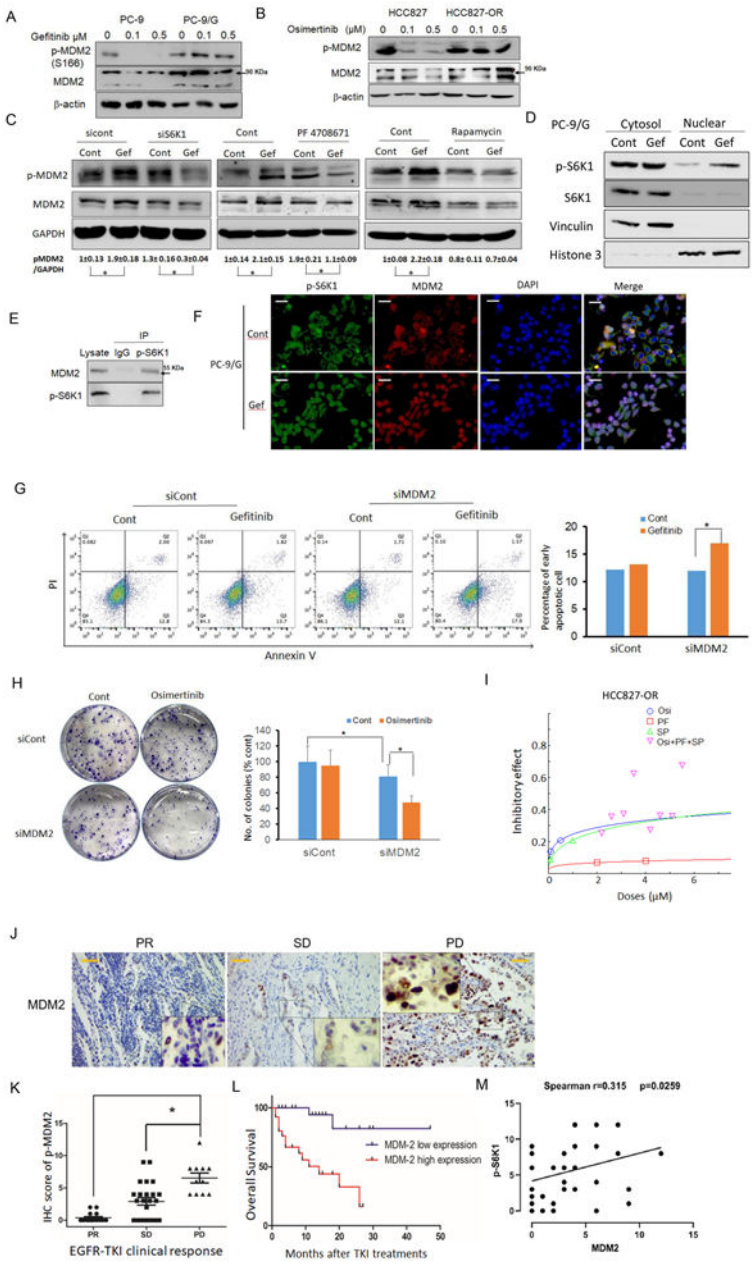

Fig.7. MDM2 is a downstream effector of S6K1-mediated TKIs resistance

(A, B) Cells were treated with EGFR-TKI for 24 hours at indicated doses and then were subject to Western-blots. **(C)** PC-9/G cells were transiently transfected with siS6K1 SMARTPOOL or scrambled control (siCont) respectively. After 24 hours of transfection, the cells were treated with or without gefitinib (0.5 μM) for 24 hours followed by Western-blots. PC-9/G cells were treated with PF-4708671 (4 μM) or rapamycin (50 nM) for 24 hours followed by Western-blots. Densitometry using Image J was used for quantification of bands. (**D**) PC-9/G cells were treated with gefitinib (0.5 μM) for 24 hours followed nuclear and cytoplasmic extraction. S6K1 and p-S6K1 protein levels were determined in cytosol and nuclear fractions, respectively. **(E)** Co-IP assay was performed in PC-9/G cells. The protein

complex was pulled down by p-S6K1 antibody or IgG followed by immunoblotting with MDM2 antibody and p-S6K1 antibody. (**F)** PC-9/G cells were treated with gefitinib (0.5 μM) followed by immunofluorescence assay. Magnification: 200×. Scale bar: 50 μm. (**G**) PC-9/G cells were transfected with siMDM2 SMARTpool or siCont respectively. After 24 hours transfection, the cells were treated with gefitinib (0.5 μM) for 48 hours and then were subject to apoptosis assay. (**H)** HCC827-OR cells were transfected with siMDM2 SMARTpool or siCont respectively. After 24 hours transfection, cells were reseeded at 1000 cells/well and cultured in the medium with or without osimertinib (0.1 μM) for 7 days. Colonies were photographed and counted. (**I**) HCC827-OR cells were treated with osimertinib alone (0.1 μM, 0.5 μM), PF alone (2 μM, 4 μM), SP-141 (0.1 μM, 1 μM), or combinations of three drugs for 24 hours. The MTT assay was used to determine cell viability. The figure of combine effects were generated by CompuSyn software. (**J**) Representative images of MDM2 staining (× 200 and × 650 magnifications) were shown based on clinical response to EGFR-TKIs. PR: partial response; SD: stable disease; PD: progressive disease. Scale bar: 50 μm. (**K**) Correlation analysis was performed between MDM2 levels and clinical responses. PR (n=16), SD (n=25), PD (n=10). (**L**) Kaplan-Meier curves were used to show overall survival of NSCLCs patients stratified based on the expression levels of MDM2. The cutoff of value of subgroups (low, high) of MDM2 expression level was the 50% percentile value. (**M**) The correlation analysis between MDM2 and p-S6K1 expression levels were shown. n=51. Spearman correlation analysis was performed. r= 0.315, P= 0.0259. Quantitative results were analyzed by Student’s t test (two groups) or one-way ANOVA (more than three groups) with $P \leq 0.05$ considered significant and are shown as mean ± SD. *P<0.05, **P<0.01.